Covalent Incorporation of Aminated Nanodiamond into an Epoxy Polymer Network

Vadym N. Mochalin,[†] Ioannis Neitzel,[†] Bastian J. M. Etzold,[†,§] Amy Peterson,[‡] Giuseppe Palmese,[‡] and Yury Gogotsi[†,*]

[†]Department of Materials Science and Engineering and A.J. Drexel Nanotechnology Institute, [‡]Department of Chemical and Biological Engineering, Drexel University, Philadelphia, Pennsylvania 19104, United States and [§]Lehrstuhl für Chemische Reaktionstechnik, Universität Erlangen-Nürnberg, 91058 Erlangen, Germany

ABSTRACT Outstanding mechanical and optical properties of diamond nanoparticles in combination with their biocompatibility have recently attracted much attention. Modification of the surface chemistry and incorporation into a polymer is required in many applications of the nanodiamond. Nanodiamond powder with reactive amino groups (~20% of the number of surface carbon atoms in each 5 nm particle) was produced in this work by covalent linking of ethylenediamine to the surface carboxyl groups *via* amide bonds. The synthesized material was reacted with epoxy resin, yielding a composite, in which nanodiamond particles are covalently incorporated into the polymer matrix. The effect of amino groups grafted on the nanodiamond on the curing chemistry of the epoxy resin was analyzed and taken into consideration. Covalently bonded nanodiamond–epoxy composites showed a three times higher hardness, 50% higher Young's modulus, and two times lower creep compared to the composites in which the nanodiamond was not chemically linked to the matrix. Aminated nanodiamond produced and characterized in the present study may also find applications beyond the composites, for example, as a drug, protein, and gene delivery platform in biology and medicine, as a solid support in chromatography and separation science, and in solid state peptide synthesis.

KEYWORDS: nanodiamond · surface chemistry · nanocomposites · epoxy · amination · hardness · Young's modulus

Nanosized diamond powder is a relatively inexpensive carbon nanomaterial produced by detonation synthesis in large volumes. It has a broad range of potential applications including selective adsorbents, lubricants and polishing compositions, additives to electrolytic and electroless deposition baths, as well as others.[1−3] Recent years have witnessed a rapid growth of interest in applications of nanodiamond (ND) in biomedicine and polymer matrix composites.[4−15] In this report, we focus on the latter application.

As-produced detonation soot contains 25−30 wt % of nanodiamond particles that are surrounded by graphene shells and amorphous carbon. Commercial-acid-purified ND is composed of particles of ~5 nm in diameter combining an inert diamond core with a large number of covalently bonded surface groups such as C═O, COOH, OH, CH_2, CH_3, (poly)aromatic fragments, *etc.*[1−3,16,17] The variety of surface groups is an inherent property of ND, offering numerous options to adjust surface chemistry yet posing potential problems. Particularly, the noncovalent interactions between these surface functional groups are thought to play a role in formation of strong ND aggregates, which make dispersion of ND into single particles a challenge.[18] In the context of composite applications, the failure to use consistent ND material with precise control of its carbon structure/hybridization and surface chemistry could be one of the reasons for contradicting reports regarding the properties of ND–polymer matrix composites. There are reports of improvements in mechanical strength,[4,6−8,11,12,15] wear resistance,[19] adhesion to metal,[5] electromagnetic shielding[13] and thermal conductivity[15,20] of polymers, as well as reports of no improvement or an unexpected degradation in properties. These discrepancies can be attributed to different and not necessarily favorable interactions of nanoparticles with the matrix. Because of its tailorable surface chemistry, ND offers many options to adjust these interactions as well as improve the dispersion in the matrix without compromising the properties of the diamond core. This is in contrast to small diameter nanotubes where chemical functionalization often alters core structure and reduces their mechanical properties.[21]

Interfacial failures, along with dispersion issues, constitute the major cause for poor performance of nanocomposites in general[22,23] and diamond–epoxy composites in particular.[24,25] To improve the interface and increase the strength of the nanocomposites, researchers attempted

* Address correspondence to gogotsi@drexel.edu.

Received for review July 2, 2011 and accepted August 10, 2011.

Published online August 10, 2011
10.1021/nn2024539

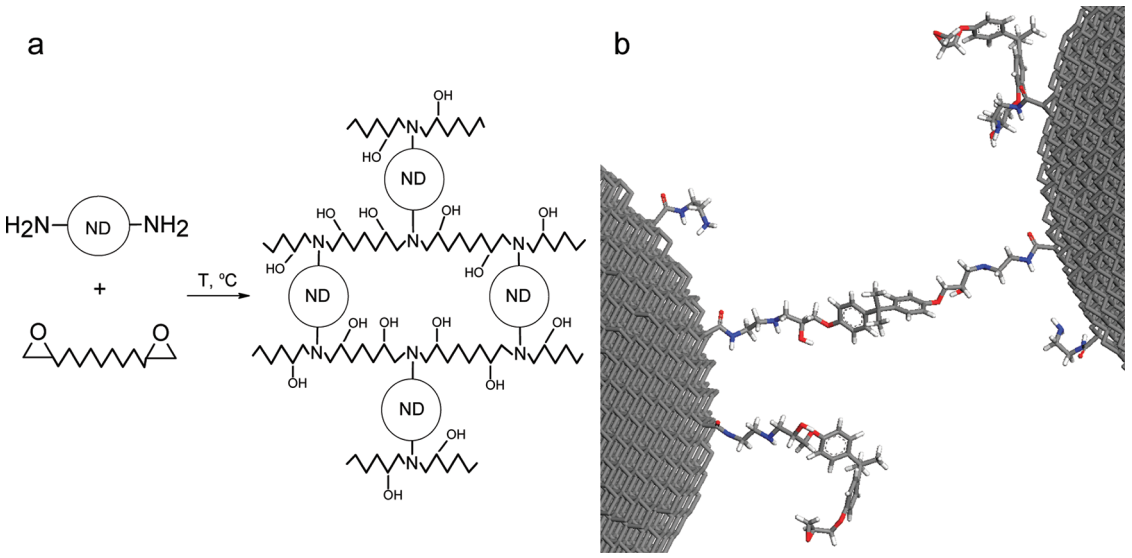

Figure 1. Schematics of covalent incorporation of aminated ND into a structure of epoxy polymer (a) and a simplified molecular model of the resulting covalently bonded composite (b), where carbon is shown in gray, oxygen in red, nitrogen in blue, and hydrogen in white. For clarity, only a few surface groups that are involved in interface formation are shown.

to form covalent bonds between different fillers and polymers. Some examples where covalent interfaces in nanocomposites were formed include single-walled or multiwalled carbon nanotubes and epoxies,[26−28] single-walled carbon nanotubes and nylon,[29] silica nanoparticles and vinyl polymers formed by reactions with different monomers such as methyl methacrylate, styrene, and glycidyl methacrylate.[30] Polymer grafting aimed at achieving better dispersion and forming covalent interfaces has been studied with ND and poly(ether ketone),[9] polyimides,[11,12] poly(*tert*-butyl) and poly(*iso*-butyl) methacrylates,[31] polystyrene, and poly(*tert*-butyl methacrylate).[32] However, there are no studies on covalent incorporation of ND in epoxy systems, which represent a large and important class of thermosetting engineering polymers used as adhesives, structural materials, coatings, and encapsulants.[33] Curing chemistry of epoxies is based on the reaction of the epoxy groups of a resin with curing agents (usually amines) at ambient or elevated temperatures. Therefore, one way to incorporate ND into the epoxy network is through covalent bond formation between amino groups attached to ND and epoxy groups of the resin (Figure 1a), resulting in the epoxy network being covalently bound to the ND particles (Figure 1b). A similar approach has been used in ref 28, where the amino-functionalized carbon nanotubes, produced by attachment of a commercial curing agent *via* diazonium chemistry, reacted with epoxy resin.

In this study, we report on the synthesis of aminated ND by linking ethylenediamine to the surface of purified carboxylated ND and its use as a reactive nanofiller to produce covalently bonded ND−epoxy composites.

RESULTS AND DISCUSSION

The wet chemistry procedure we used in this work to produce aminated ND is a modified version of the procedure that was used for linking octadecylamine to ND *via* amide bond.[35] In this work we attached ethylenediamine (EDA) (Scheme 1). To produce covalently bonded ND−epoxy composites, it is necessary to have the amino groups covalently attached to the ND surface, not simply adsorbed onto it. Therefore, special attention was paid to establishing the fact of chemical bonding between the EDA and ND. To distinguish between the adsorbed and chemically bonded EDA, we were looking for evidence of an amide bond in ND−NH_2, which could only be formed in the reaction between carboxylic groups of ND−COOH and amino groups of EDA (Scheme 1). This evidence is provided by a comparison of FTIR spectra of ND−COOH and ND−NH_2 in Figure 2.

An intense peak at 1665 cm^{-1} observed in ND−NH_2 and absent in ND−COOH corresponds to a somewhat blue-shifted amide I band of secondary amides.[36] Amide I is a strong band characteristic of all amides that originates from C═O stretch vibrations blue-shifted by electronegative N atom and red-shifted by resonance with a lone electron pair of the N atom and by hydrogen bonding. A distinctive peak at 1535 cm^{-1}, which is observed in the IR spectrum of ND−NH_2 and absent in the spectrum of ND−COOH (Figure 2b), corresponds to the amide II band in a secondary amide. Amide II, a mixture of the C−N stretch and the N−H bend vibrations, is positioned at 1550 ± 20 cm^{-1} in secondary amides.[36] There are also hints of the amide III band in the spectrum of ND−NH_2 as evidenced by

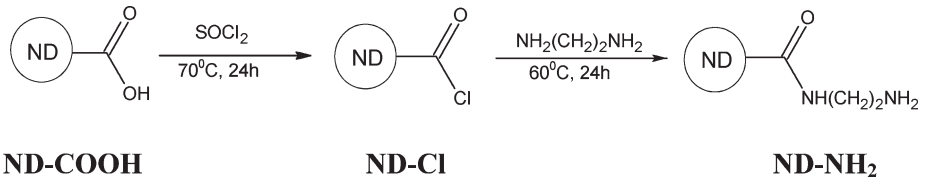

Scheme 1. Sequence of reactions used for synthesis of ND−NH_2.

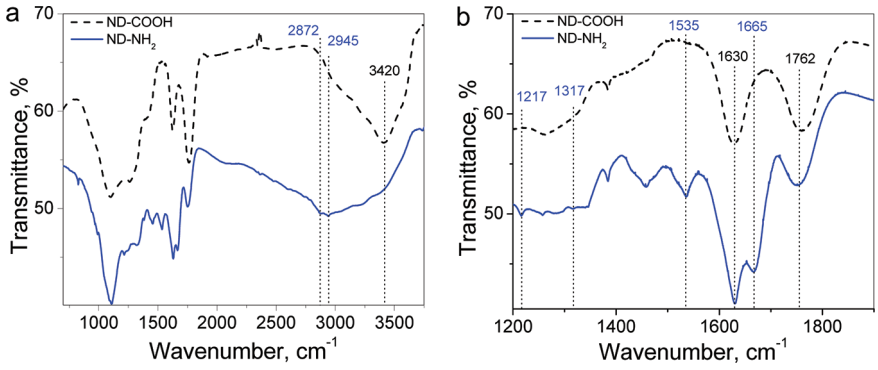

Figure 2. FTIR spectra of ND−COOH and ND−NH_2 recorded at 4 cm^{-1} (a) and 0.5 cm^{-1} (b) resolution. Read text for peak identification.

the peaks in the range of 1217−1317 cm^{-1} absent in ND−COOH. However, these peaks are of low intensity, thus unambiguous assignment is difficult. The 1630 cm^{-1} peak observed in both ND−COOH and ND−NH_2 can be assigned to the bending mode of O−H or N−H bonds.

Comparison of the ND−NH_2 and ND−COOH FTIR spectra in the higher frequency range also reveals differences suggesting the presence of N−H and C−H stretch vibrations in ND−NH_2. In general, the maximum of intensity in the 2800−3500 cm^{-1} range is red-shifted in ND−NH_2 (Figure 2a). This shift is due to the overlapping bands of the N−H stretch (which in secondary amides should be at 3160 or 3300 cm^{-1}, depending on *cis* or *trans* position of N−H relative to C═O[36]) and C−H stretch vibrations in the two CH_2 groups of ND−NH_2 (see Scheme 1). Small peaks at 2872 and 2945 cm^{-1} absent in ND−COOH and barely distinguishable atop a strong N−H and O−H stretch background broadened due to hydrogen bonding in ND−NH_2 correspond to the C−H stretch vibrations. Finally, there is a strong peak of C═O stretch (1762 cm^{-1}) in both materials, suggesting the presence of non-amide carbonyl species (carboxylic acids, ketones, esters, *etc.*) in ND−NH_2, that is, incomplete coverage of the ND−NH_2 surface with the amides, which is not surprising, but needs to be noted for interpretation of further results.

Thus, IR data provide crucial evidence of covalent attachment of EDA to ND according to Scheme 1. The resulting ND−NH_2 is expected to possess more basic properties due to the presence of free amino groups in contrast to ND−COOH, which has acidic properties due to the surface carboxylic groups. Indeed, a comparison of ζ-potential and particle size *versus* pH of ND−NH_2 and ND−COOH in aqueous dispersions (Figure 3) reveals a dramatic difference in the acid−base characteristics of these two materials.

In neutral environment (pH = 7), ζ-potential of ND−COOH is about −30 mV, right at the verge of the potential required to maintain dispersion stability. The negative sign is due to the surface $-COO^-$ formed as a result of dissociation of carboxylic groups. At pH > 7, where the equilibrium ND−COOH ⇌ ND-COO^- + H^+ shifts to the right, ζ-potential of ND−COOH becomes slightly more negative, and the particle size is further reduced, resulting in a more stable ND colloidal solution, and *vice versa*, when pH is reduced and the equilibrium shifted toward the left, ζ-potential becomes less negative, the ND−COOH aggregates, and the dispersion eventually collapses (Figure 3a). ND−NH_2 behavior is rather opposite. In neutral aqueous environment, it has a positive and small (≪30 mV) value of ζ-potential, thus dispersions of ND−NH_2 at pH ∼7 are not stable (Figure 3b). The small positive values of ζ-potential of ND−NH_2 are in agreement with an incomplete conversion of COOH surface groups into amides, as evidenced by IR spectra (Figure 2). Because of the presence of both carboxylic and amino groups on the surface, ND−NH_2 is an amphoteric material and demonstrates basic properties in acidic environment due to the protonation of amino groups (ND−NH_2 + H^+ ⇌ ND−NH_3^+). The protonation results in more positive ζ-potential at lower pH reaching 25−27 mV at a pH between 2 and 3 (Figure 3b) and in a corresponding reduction in particle size and increase in stability of the colloidal solution.

Thermogravimetric analysis (Figure 4) provides additional evidence of amino group presence on the ND's

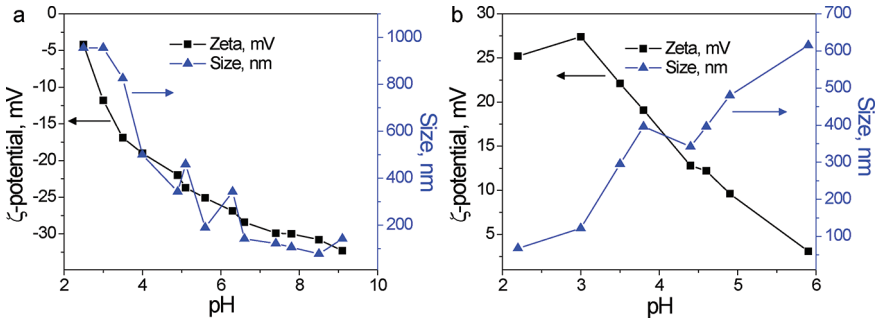

Figure 3. Particle size (zeta-average diameter) and ζ-potential of ND−COOH (a) and ND−NH_2 (b) in 0.1 wt % aqueous dispersions as a function of pH.

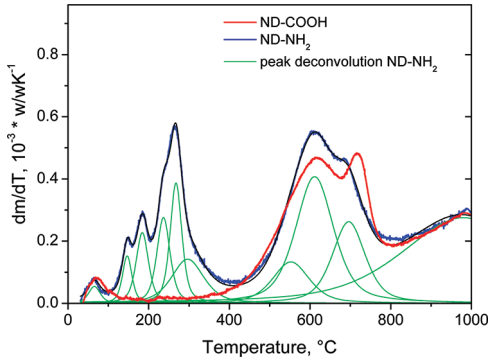

Figure 4. DTG curves of ND−COOH and ND−NH_2.

surface. A large peak at 150−350 °C seen on the differential thermogravimetric (DTG) curve of ND−NH_2 and absent on the curve of ND−COOH can be deconvoluted into five peaks with maxima at 145, 185, 235, 265, and 295 °C, which were shown in the literature to be characteristic for amino groups.[37,38] Carboxylic groups, which normally decompose in the range of 250−400 °C,[39−43] have little or no contribution to this peak as evidenced by the curve of ND−COOH.

While it is unclear why ND−COOH shows no COOH decomposition peak, it can be hypothesized that the majority of COOH groups on the ND surface are located close to each other and form anhydrides, eliminating H_2O when ND−COOH is dried or heated.

The decomposition of ND−COOH shows two pronounced peaks with maxima at 620 and 700 °C and a minor mass loss above 900 °C. The second peak and the mass loss above 900 °C correspond to anhydrides, lactones, phenols, ethers, or carbonyls (in the order of increasing decomposition temperature), while the first peak at 530−620 °C present on the DTG curves of both ND−COOH and ND−NH_2 (Figure 4) corresponds to anhydrides.

Thus, combined results of IR spectroscopy, DTG, ζ-potential, and particle size *versus* pH measurements confirm that ND−NH_2 produced according to Scheme 1 has amino groups chemically bonded to its surface.

This material was used for covalent incorporation into Epon828 epoxy resin. Assuming that ND−NH_2 will react with epoxy in a way similar to other amine curing agents, we expected the formation of covalently bonded ND−epoxy composite as shown in Figure 1.

In order to monitor this reaction and estimate the number of ND−NH_2 amino groups reacted with Epon828, we performed *in situ* DSC curing experiments. Representative DSC curves for neat Epon828 as well as Epon828 with different amounts of ND−COOH and ND−NH_2 are shown in Figure 5a. To determine the number of reactive amino groups in ND−NH_2, we first ran seven samples of Epon828 mixed with 0−50 pph PACM. The measured heat of curing was plotted against the number of amino groups, derived from the compositions of these samples (similar to the procedure described in ref 34). The estimated heat of curing obtained by averaging the values corresponding to the compositions at which all epoxy groups in the system have reacted (>28 pph PACM) was equal to 550 ± 50 J/g of Epon 828 or 104 ± 9 kJ/mol of epoxy groups.

Then, the samples of Epon828 with ND were measured (no PACM added), the heat evolved was integrated in the range of 60−163 °C, and the heat of curing per 1 mol of epoxy groups was used to determine the content of reactive amino groups on the ND. Assuming that all ND particles are spherical having a 5 nm diameter and the number of NH_2 groups attached to ND is equal to the number of reacted NH_2 groups (though in fact the former might be higher), we conclude that ~1/5 of surface carbon atoms of ND−NH_2 are terminated with reactive amino groups (Table 1).

As discussed above, the incomplete NH_2 coverage was found in FTIR (Figure 2), demonstrated by ζ-potential and particle size titration (Figure 3), and is generally anticipated given the steric limitations of the reactions in Scheme 1. In addition, not all available amino groups of ND−NH_2 are expected to react with epoxy; therefore, ~20% of the surface atoms are a reasonable estimate of the amino group coverage in our ND−NH_2. To our knowledge, this is the first time any kind of functional groups on the ND surface has been quantitatively measured.

Glass transition temperatures (T_g) of the samples measured after they were heated to 180 °C increased

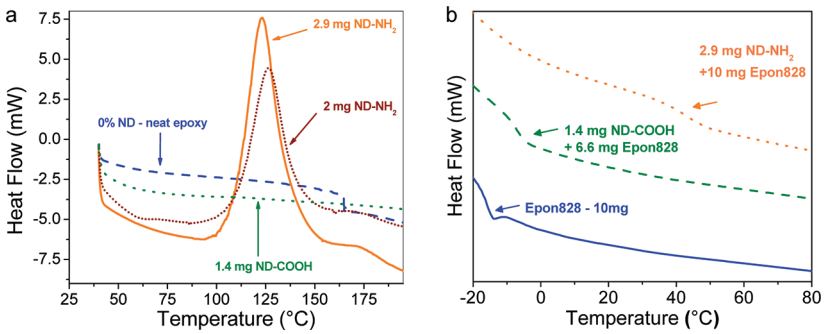

Figure 5. DSC curves for pure Epon828 and Epon828 mixed with different amounts of ND−COOH and ND−NH_2. Heating rate 10 °C/min. (a) Heat evolved in reaction between the epoxy resin and nanodiamond; (b) glass transition temperatures for the same samples after they were heated to 180 °C to complete reactions between nanodiamond and epoxy.

TABLE 1. Content of Surface Amino Groups of ND−NH_2 Reacted with Epon828 As Measured by Integration of Heat Evolved in DSC Experiments in the Range of 60−163 °C

sample composition (mg)					
ND (type)	Epon828	$heat_{60-163\ °C}$ ($J/g_{Epon828}$)	amine equivalent weight of ND (g/mol)[a]	NH_2-terminated surface atoms (%)[b]	surface density of reactive NH_2 groups ($groups/nm^2$)[c]
0	5.6	0.0	0.0	0.0	0.0
1.4 (ND−COOH)	6.6	0.0	0.0	0.0	0.0
2.9 (ND−NH_2)	10	151.7	151.3	22.7	4.5
2 (ND−NH_2)	8.5	119.5	155.8	22.0	4.4
2.8 (ND−NH_2)	7.3	157.4	192.8	17.8	3.5

[a] The molecular weight of ND per amine hydrogen, calculated with the assumption that both hydrogen atoms in NH_2 group react with epoxy. [b] Calculated for a 5 nm diameter ND particle composed of 11 686 C atoms, 1560 of which are exposed on the surface. [c] Calculated as the number of −NH_2-terminated surface atoms divided by the surface area of a single 5 nm diameter ND particle (78.5 nm^2).

with the addition of ND−COOH and ND−NH_2 (Figure 5b). With no ND added, the T_g of Epon828 is −15.21 °C; with addition of ND−COOH, it is slightly higher (−10.68 °C) and is much higher (42.31 °C) when ND−NH_2 was added. The high T_g observed when ND−NH_2 was used in comparison to much lower values obtained for Epon828 and Epon828 with ND−COOH clearly indicates that ND−NH_2 cross-links the resin in these conditions, whereas ND−COOH does not. These experiments show that potentially ND−NH_2 can be used to completely replace PACM for epoxy curing.

Our final goal was to demonstrate that the addition of ND−NH_2, which forms strong covalent C−N bonds with epoxy, results in better mechanical properties as compared to the addition of ND−COOH. However, since ND−NH_2 brings additional reactive groups into the system, it will interfere with the epoxy resin/curing agent stoichiometry, which must be taken into consideration. This issue was recently pointed out for carbon nanotubes[33] and has also been observed in traditional composites.[44] The interference of nonfunctionalized and functionalized carbon nanotubes with epoxy curing chemistry has been attracting increasing attention, but we are not aware of any prior studies of ND interference with epoxy curing chemistry. Palmese and McCullough have demonstrated that T_g and flexural modulus of Epon828 cured with PACM are very sensitive to the resin:curing agent ratio,[34] with a flex modulus (measured at 30 °C) peaking at 18 pph of PACM (3.2 GPa) and sharply declining when PACM content deviates from 18 pph in either direction. Thus, at the stoichiometric composition (28 pph PACM), the flex modulus of the Epon828−PACM cured polymer is lower (2.3 GPa) compared to nonstoichiometric composition with 18 pph PACM.[34] To compensate for the additional amino groups brought with ND−NH_2, the amount of PACM must be reduced compared to a stoichiometric amount in the Epon828−PACM system. The improvement provided by covalent incorporation of ND with accounting for the additional amino groups of ND−NH_2 was demonstrated by comparison of the nanoindentation data for the composites in which ND−NH_2 was used against the composites prepared with ND−COOH. Figure 6 shows representative nanoindentation curves for Epon828−ND−COOH and Epon828−ND−NH_2 composites cured with 11 pph PACM. At this composition, with no ND added, the cured polymer had a low hardness and Young's modulus, which is not surprising given how far below the optimal composition we were. Mechanical properties quickly recover due to the addition of ND. At moderate concentrations, both ND−NH_2 and ND−COOH restore the mechanical properties, however, the improvement

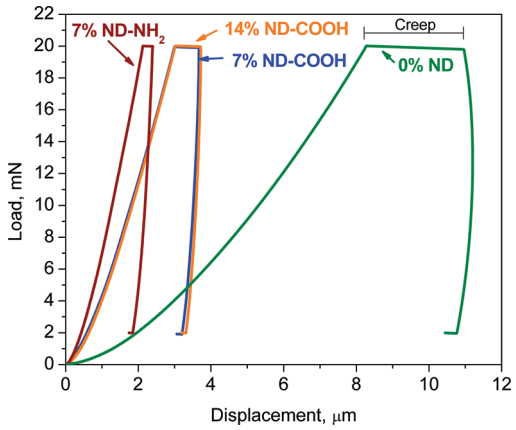

Figure 6. Load–displacement curves of neat epoxy and ND–Epon828 composites with different concentrations of ND–COOH and ND–NH_2. The concentration of PACM in the system was kept constant at 11 pph for all samples.

is much more pronounced for ND–NH_2, as evidenced by a comparison of the curves for 7 wt % ND–COOH and 7 wt % ND–NH_2 in Figure 6. Since the contribution of all nonspecific factors, that is, those not related directly to surface chemistry of ND, such as superior hardness and Young's modulus of the ND itself, an increased viscosity and thermal conductivity of the system upon addition of ND should be similar no matter which ND was used, we assign the observed 180% higher hardness, 50% higher Young's modulus, and 150% reduced creep of the composite with 7 wt % of ND–NH_2 as compared to 7 wt % ND–COOH (see also Table 2) to the effect of covalent incorporation of ND–NH_2 into the resulting polymer network.

This significant improvement could only be achieved with ND–NH_2; even at two times higher concentration, ND–COOH did not bring the mechanical properties of the composite close to that made with 7 wt % of ND–NH_2 (Figure 6, Table 2). However, it is possible that even better properties can be achieved in the ND–NH_2–Epon828–PACM system. Based on data of ref 34, we expected the maximum in Young's modulus of our ND–epoxy composites to be at PACM concentration below 18 pph to compensate for the introduction of the additional reactive amino groups of ND–NH_2. In fact, these amino groups of ND–NH_2 add a second composition variable (in addition to Epon828/PACM ratio). Although the maximum in flexural modulus in the Epon828–PACM system was achieved at 18 pph of PACM,[34] it is not known whether the same total content of amino groups (PACM and ND–NH_2) will maximize the Young's modulus in the ND–NH_2–Epon828–PACM composite because the presence of ND particles themselves may change the dependence of mechanical properties on composition. Therefore, more extensive studies are required to maximize properties of ND–NH_2–Epon828–PACM composites, accounting for additionally introduced amino groups.

TABLE 2. Mechanical Properties of ND–Epon828 Composites with Different Concentrations of ND–COOH and ND–NH_2 Derived from Nanoindentation Curves (Concentration of PACM in All Samples Was Kept Constant at 11 pph)

ND content (wt %) and type	Young's modulus (GPa)	hardness (MPa)	creep (nm)
0 ND	0.27 ± 0.02	0.4 ± 0.1	2649
7% ND–COOH	2.0 ± 0.4	30 ± 10	667
7% ND–NH_2	3.0 ± 0.4	90 ± 30	266
14% ND–COOH	1.5 ± 0.2	16 ± 4	671

Aminated ND produced in this work will find many other applications. Free amino groups on its surface can be used for conjugation of proteins, genetic material, and drugs *via* well-developed bioconjugation techniques.[45,46] A very interesting application for aminated ND will be its use as a support in Merrifield's solid state peptide synthesis, where polymer microbeads are currently used.[47] ND is studied as a solid phase in chromatography[48] and adsorption,[49] where ND–NH_2 can provide selectivity toward certain analytes. Due to its positive ζ-potential in neutral aqueous environment, aminated nanodiamond can also be used along with ND–COOH in layer-by-layer deposition of nanodiamond-containing materials.

CONCLUSIONS

Nanodiamond particles with amino-group-terminated surfaces have been synthesized by a wet chemistry technique through amide bond formation between acyl chloride groups on the nanodiamond and one of the amino groups of ethylenediamine. Covalent attachment of the diamine has been confirmed by observation of amide bands in the IR spectrum. The aminated material demonstrates amphoteric properties due to NH_2 and COOH groups exposed on its surface. As a base, it shows a high positive ζ-potential and an improved colloidal stability at low pH, in contrast to the initial ND–COOH, which has a high negative ζ-potential and better dispersion stability at high pH. On the basis of DSC studies of reactions between the ND–NH_2 and Epon828, we determined that the content of amino groups in the aminated nanodiamond is about 20% of the number of surface carbon atoms on each 5 nm diamond particle.

Reaction of aminated ND with epoxy resin results in covalent incorporation of the ND into a polymer network. It was found to be important to reduce the content of the curing agent added to account for amino groups on the ND surface. At higher concentrations, ND–NH_2 can potentially provide enough NH_2 groups to completely replace the curing agent.

The resulting ND–Epon828 composite with 11 pph PACM and 7 wt % of ND–NH_2 demonstrated ~200 times higher hardness, ~10 times higher Young's modulus, and ~10 times lower creep in comparison to Epon828 cured with 11 pph PACM and no ND added.

By contrast, Epon828 with 11 pph PACM and 7 wt % of ND−COOH showed ~75 times higher hardness, ~7 times higher Young's modulus, and ~4 times lower creep in same comparison. Thus, the improvements in Young's moduli and hardness values of ND−COOH containing composites are substantially less, taking into consideration that even doubled amount of ND−COOH (14 wt %) has not resulted in further improvement of properties. This emphasizes the advantages of covalent incorporation of the nanofiller.

The technique of covalent incorporation developed in this study can be applied with proper modification to other polymer systems, producing covalently bonded polymer−ND composites with superior mechanical properties and enhanced thermal conductivity.

MATERIALS AND METHODS

Materials. Nanodiamond powder UD90 produced by detonation synthesis was supplied by NanoBlox, Inc., USA. The powder was extensively characterized and purified from nondiamond carbon by oxidation in air and reflux in 35 wt % aqueous HCl to remove traces of metals and metal oxides. Purification of UD90 and characterization of the purified ND was reported elsewhere.[16] After the HCl reflux, the ND was allowed to settle to the bottom of the flask. The excess HCl was removed; ND powder was separated by centrifugation, rinsed with DI water until neutral pH, and then dried in an oven at 110 °C overnight. This purified ND with acidic groups on the surface labeled as ND−COOH hereafter was a starting material for subsequent functionalization. We used thionyl chloride ≥99.0% purum (Fluka), methanol 99.8% anhydrous (Sigma-Aldrich), tetrahydrofuran (THF) 99.85% ExtraDry (Acros Organics), ethylenediamine (EDA) SigmaUltra (Sigma-Aldrich), and *N*,*N*-dimethylformamide (DMF) 99.8% anhydrous (Sigma-Aldrich). All reagents were used without additional purification.

Epoxy resin Epon828 (diglycidyl ether of bisphenol A) with an average MW = 377 g/mol as specified by the manufacturer and curing agent PACM (bis-*p*-aminocyclohexyl methane) were supplied by Hexion and Air Products, Inc. The cure chemistry and effects of composition on properties of this epoxy system have been described elsewhere.[34]

Synthesis of Aminated ND. Two reaction steps in which ND−COOH is converted into the NH_2-terminated product (ND−NH_2) are presented in Scheme 1.

Synthesis of ND Acylchloride Derivative (ND−Cl). Approximately 1.5 g of ND−COOH was mixed with 50 mL of $SOCl_2$ and 0.5 mL of anhydrous DMF (catalyst) in a round-bottom 100 mL glass flask with a Teflon-coated magnetic stirrer bar. The flask was closed with a stopper and sonicated in an ultrasound bath until all visible agglomerates of nanodiamond were destroyed. Then, the flask was connected to a reflux condenser closed with a desiccating tube (Drierite) and heated under reflux at 70 °C for 24 h. After cooling to room temperature, the excess $SOCl_2$ was removed by vacuum distillation at a temperature ≤50 °C to prevent its thermal decomposition. The solid content that remained in the flask after removing $SOCl_2$ was rinsed five times with 50 mL of anhydrous THF. After rinsing, the ND−Cl powder (Scheme 1) was left to precipitate, the flask was open, and excess THF removed by decantation. Then the flask was transferred into a desiccator with Drierite and left under vacuum at room temperature overnight to dry the ND−Cl powder.

Synthesis of ND Amino Derivative (ND−NH_2). Approximately 1.5 g of ND−Cl was mixed with 50 mL of anhydrous EDA in a round-bottom 100 mL flask with a Teflon-coated magnetic stirrer bar. The flask was closed with a stopper and sonicated in an ultrasound bath until no nanodiamond agglomerates could be seen. Next, the flask was connected to a reflux condenser closed with a desiccating tube (Drierite) and heated under reflux at 60 °C for 24 h. After cooling to room temperature and precipitation of the powder, excess EDA was removed with a pipet and the powder was rinsed five times, every time with 50 mL of fresh anhydrous THF, in order to remove any traces of adsorbed EDA. When the last rinse was completed, a few drops from the THF layer were mixed with 10 mL of DI water and the pH of this solution was measured with indicator paper to ensure complete washing out of the adsorbed EDA. The resulting ND−NH_2 was split in two parts. One part was transferred onto a watch glass and dried at room temperature for subsequent characterization. Another part was stored in the form of THF suspension to suppress agglomeration and was kept under continuous vigorous stirring for the entire period of time between synthesis and utilization of ND−NH_2 for composite manufacturing. This latter part was used to produce ND−epoxy composites. The concentration of ND in the suspension was measured by weight after THF evaporation.

Manufacturing of ND−Epoxy Composites. For each composite, 3 g of Epon828 was dissolved in 4.5 g of THF. A predetermined amount of ND−COOH or ND−NH_2 dispersed in THF was added to the solution. The resulting mixtures were sonicated and then stirred on a hot plate for 24 h at 50 °C using a Teflon-coated stirrer bar, followed by THF evaporation for 24 h. Then 11 pph of the curing agent PACM was added to the Epon828−ND mixture (pph stands for parts per hundred of epoxy, i.e., 11 pph means 11 g of PACM added to 100 g of Epon828). All samples were cured for 2 h at 80 °C followed by 2 h at 165 °C according to a standard curing procedure for this epoxy system.[34]

Preparation of Samples for Differential Scanning Calorimetry (DSC). Few drops of ND−COOH or ND−NH_2 suspensions in THF (or of pure PACM for reference samples) were placed in an aluminum DSC pan. The weight of ND in the pan determined after evaporation of THF was in the range of 2−4 mg. After that, 5−10 mg of Epon828 was added to a pan and precisely measured by weighing the pan again before placing it into the DSC chamber, where it was heated at 10 °C/min in N_2 flow to monitor the curing process *in situ*. The heat of reaction was calculated by integration of DSC peaks in the range of 60−163 °C.

Characterization. IR spectra of ND were recorded in KBr pellets with the FTIR spectrometer Excalibur FTS-3000 (Varian, USA) at 4 and 0.5 cm^{-1} resolution. Particle size and ζ-potential of ND were measured at 20 °C in back scatter geometry using a Malvern Zetasizer Nano ZS (Malvern Instruments Ltd., UK) equipped with a 10 mW He−Ne laser (633 nm) and an MPT-2 autotitrator.

TGA measurements were performed with ~10 mg of material in an alumina pan using a Q50 thermogravimetric analyzer (TA Instruments, USA). All measurements were performed in N_2 atmosphere (Airgas, USA, nitrogen, compressed, 2.2, UN1066) after 2 h of flushing the setup with N_2 at room temperature to ensure complete removal of air. The weight loss was recorded for a temperature ramp from ambient to 1000 °C (5 °C/min). From ~10 000 points, the temperature differential of the mass was calculated as

$$\frac{dm_i/m_0}{dT} = \frac{m_{i+1} - m_{i-1}}{T_{i+1} - T_{i-1}} \frac{1}{m_0}\left[\frac{w/w}{K}\right] \quad (1)$$

where T = temperature [K], m = mass [kg], m_0 = initial mass [kg], i = data point index.

For plotting, the differential curves calculated by eq 1 were smoothened with the Savitzky−Golay filter (50 data points, second order polynomial) using OriginPro 8.5.

The amount of reactive amino groups on the surface of ND−NH_2 particles was estimated using a Q2000 differential scanning calorimeter (DSC) (TA Instruments, USA). All

measurements were performed in the temperature range of 40−200 °C with a heating rate of 10 °C/min. The amount of heat evolved, measured in the temperature range of 60−163 °C, was used to estimate the number of the reacted amino groups of ND−NH_2. To measure glass transition temperatures (T_g), the DSC curves of the cured epoxy samples were recorded in the temperature range of −30 to 180 °C.

Nanoindentation measurements were performed using a NanoIndenter XP (MTS Corp., USA) equipped with a continuous stiffness measurement (CSM) attachment. All measurements were done with a 5 μm radius spherical indenter at a constant strain rate of 0.03 s^{-1}. The tests were stopped at a maximum load of 20 mN followed by a 30 s hold segment to measure creep.

Acknowledgment. This work was supported by NSF grant CMMI-0927963. B.E. acknowledges the financial support from the Alexander von Humboldt Foundation. The authors acknowledge access to FTIR spectrometer and Nanoindenter provided by Centralized Research Facilities, College of Engineering, Drexel University.

REFERENCES AND NOTES

1. Shenderova, O. A.; McGuire, G. Nanocrystalline Diamond. In *Nanomaterials Handbook*; Gogotsi, Y., Ed.; CRC Taylor and Francis Group: Boca Raton, FL, 2006; pp 203−237.
2. Shenderova, O. A.; Gruen, D. M. *Ultrananocrystalline Diamond: Synthesis, Properties, and Applications*; William Andrew Publishing: Norwich, NY, 2006.
3. Ho, D. *Nanodiamond Applications in Biology and Nanoscale Medicine*; Springer: New York, 2010; p 286.
4. Behler, K. D.; Stravato, A.; Mochalin, V.; Korneva, G.; Yushin, G.; Gogotsi, Y. Nanodiamond−Polymer Composite Fibers and Coatings. *ACS Nano* **2009**, *3*, 363–369.
5. Stravato, A.; Knight, R.; Mochalin, V.; Picardi, S. C. HVOF-Sprayed Nylon-11 + Nanodiamond Composite Coatings: Production & Characterization. *J. Therm. Spray Technol.* **2008**, *17*, 812–817.
6. Zhang, Q.; Mochalin, V. N.; Neitzel, I.; Knoke, I. Y.; Han, J.; Klug, C. A.; Zhou, J. G.; Lelkes, P. I.; Gogotsi, Y. Fluorescent PLLA-Nanodiamond Composites for Bone Tissue Engineering. *Biomaterials* **2011**, *32*, 87–94.
7. Maitra, U.; Prasad, K. E.; Ramamurty, U.; Rao, C. N. R. Mechanical Properties of Nanodiamond-Reinforced Polymer-Matrix Composites. *Solid State Commun.* **2009**, *149*, 1693–1697.
8. Prasad, K. E.; Das, B.; Maitra, U.; Ramamurty, U.; Rao, C. N. R. Extraordinary Synergy in the Mechanical Properties of Polymer Matrix Composites Reinforced with 2 Nanocarbons. *Proc. Natl. Acad. Sci. U.S.A.* **2009**, *106*, 13186–13189.
9. Wang, D. H.; Tan, L. S.; Huang, H. J.; Dai, L. M.; Osawa, E. *In-Situ* Nanocomposite Synthesis: Arylcarbonylation and Grafting of Primary Diamond Nanoparticles with a Poly(ether-ketone) in Polyphosphoric Acid. *Macromolecules* **2009**, *42*, 114–124.
10. Wang, H. D.; Yang, Q. Q.; Niu, C. H. Functionalization of Nanodiamond Particles with *N,O*-Carboxymethyl Chitosan. *Diamond Relat. Mater.* **2010**, *19*, 441–444.
11. Zhang, Q.; Naito, K.; Tanaka, Y.; Kagawa, Y. Grafting Polyimides from Nanodiamonds. *Macromolecules* **2008**, *41*, 536–538.
12. Zhang, Q.; Naito, K.; Tanaka, Y.; Kagawa, Y. Polyimide/Diamond Nanocomposites: Microstructure and Indentation Behavior. *Macromol. Rapid Commun.* **2007**, *28*, 2069–2073.
13. Shenderova, O.; Jones, C.; Borjanovic, V.; Hens, S.; Cunningham, G.; Moseenkov, S.; Kuznetsov, V.; McGuire, G. Detonation Nanodiamond and Onion-like Carbon: Applications in Composites. *Phys. Status Solidi A* **2008**, *205*, 2245–2251.
14. Spitalsky, Z.; Kromka, A.; Matejka, L.; Cernoch, P.; Kovarova, J.; Kotek, J.; Slouf, M. Effect of Nanodiamond Particles on Properties of Epoxy Composites. *Adv. Compos. Lett.* **2008**, *17*, 29–34.
15. Neitzel, I.; Mochalin, V.; Knoke, I.; Palmese, G. R.; Gogotsi, Y. Mechanical Properties of Epoxy Composites with High Contents of Nanodiamond. *Compos. Sci. Technol.* **2011**, *71*, 710–716.
16. Osswald, S.; Yushin, G.; Mochalin, V.; Kucheyev, S. O.; Gogotsi, Y. Control of sp^2/sp^3 Carbon Ratio and Surface Chemistry of Nanodiamond Powders by Selective Oxidation in Air. *J. Am. Chem. Soc.* **2006**, *128*, 11635–11642.
17. Mochalin, V.; Osswald, S.; Gogotsi, Y. Contribution of Functional Groups to the Raman Spectrum of Nanodiamond Powders. *Chem. Mater.* **2009**, *21*, 273–279.
18. Pentecost, A.; Gour, S.; Mochalin, V.; Knoke, I.; Gogotsi, Y. Deaggregation of Nanodiamond Powders Using Salt- and Sugar-Assisted Milling. *ACS Appl. Mater. Interfaces* **2010**, *2*, 3289–3294.
19. Lee, J.-Y.; Lim, D.-S. Tribological Behavior of PTFE Film with Nanodiamond. *Surf. Coat. Technol.* **2004**, *188−189*, 534–538.
20. Shenderova, O.; Tyler, T.; Cunningham, G.; Ray, M.; Walsh, J.; Casulli, M.; Hens, S.; McGuire, G.; Kuznetsov, V.; Lipa, S. Nanodiamond and Onion-like Carbon Polymer Nanocomposites. *Diamond Relat. Mater.* **2007**, *16*, 1213–1217.
21. Garg, A.; Sinnott, S. B. Effect of Chemical Functionalization on the Mechanical Properties of Carbon Nanotubes. *Chem. Phys. Lett.* **1998**, *295*, 273–278.
22. Winey, K. I.; Vaia, R. A. Polymer Nanocomposites. *MRS Bull.* **2007**, *32*, 314–319.
23. Advani, S. G. *Processing and Properties of Nanocomposites*; World Scientific Publishing Company: River Edge, NJ, 2006; p 460.
24. Monteiro, S. N.; de Menezes, G. W.; Bobrovnitchii, G. S.; Skury, A. L. D.; Rodriguez, R. J. S.; d'Almeida, J. R. M. Structure and Mechanical Properties of Composites with Diamond Particles Dispersed into Modified Epoxy Matrix. *Diamond Relat. Mater.* **2007**, *16*, 974–977.
25. d'Almeida, J. R. M.; Monteiro, S. N.; Menezes, G. W.; Rodriguez, R. J. S. Diamond−Epoxy Composites. *J. Reinf. Plast. Compos.* **2007**, *26*, 321–330.
26. Zhu, J.; Peng, H. Q.; Rodriguez-Macias, F.; Margrave, J. L.; Khabashesku, V. N.; Imam, A. M.; Lozano, K.; Barrera, E. V. Reinforcing Epoxy Polymer Composites through Covalent Integration of Functionalized Nanotubes. *Adv. Funct. Mater.* **2004**, *14*, 643–648.
27. Baudot, C.; Tan, C. M.; Kong, J. C. FTIR Spectroscopy as a Tool for Nano-material Characterization. *Infrared Phys. Technol.* **2010**, *53*, 434–438.
28. Wang, S. R.; Liang, Z. Y.; Liu, T.; Wang, B.; Zhang, C. Effective Amino-Functionalization of Carbon Nanotubes for Reinforcing Epoxy Polymer Composites. *Nanotechnology* **2006**, *17*, 1551–1557.
29. Khabashesku, V. N.; Margrave, J. L.; Barrera, E. V. Functionalized Carbon Nanotubes and Nanodiamonds for Engineering and Biomedical Applications. *Diamond Relat. Mater.* **2005**, *14*, 859–866.
30. Taniguchi, Y.; Shirai, K.; Saitoh, H.; Yamauchi, T.; Tsubokawa, N. Postgrafting of Vinyl Polymers onto Hyperbranched Poly(amidoamine)-Grafted Nano-Sized Silica Surface. *Polymer* **2005**, *46*, 2541–2547.
31. Angadi, M. A.; Watanabe, T.; Bodapati, A.; Xiao, X. C.; Auciello, O.; Carlisle, J. A.; Eastman, J. A.; Keblinski, P.; Schelling, P. K.; Phillpot, S. R. Thermal Transport and Grain Boundary Conductance in Ultrananocrystalline Diamond Thin Films. *J. Appl. Phys.* **2006**, 99.
32. Cheng, J. L.; He, J. P.; Li, C. X.; Yang, Y. L. Facile Approach To Functionalize Nanodiamond Particles with V-Shaped Polymer Brushes. *Chem. Mater.* **2008**, *20*, 4224–4230.
33. Pascault, J.-P.; Williams, R. J. J. *Epoxy Polymers: New Materials and Innovations*; Wiley-VCH: Weinheim, Germany, 2010; p 387.
34. Palmese, G. R.; McCullough, R. L. Effect of Epoxy−Amine Stoichiometry on Cured Resin Material Properties. *J. Appl. Polym. Sci.* **1992**, *46*, 1863–1873.
35. Mochalin, V. N.; Gogotsi, Y. Wet Chemistry Route to Hydrophobic Blue Fluorescent Nanodiamond. *J. Am. Chem. Soc.* **2009**, *131*, 4594–4595.
36. Mayo, D.; Miller, F. A.; Hannah, R. W. *Course Notes on the Interpretation of Infrared and Raman Spectra*; John Wiley & Sons, Inc.: New York, 2004.

37. Damian, C. M.; Pandele, A. M.; Iovu, H. Ethylenediamine Functionalization Effect on the Thermo-Mechanical Properties of Epoxy Nanocomposites Reinforced with Multiwall Carbon Nanotubes. *UPB Sci. Bull., Ser. B* **2010**, *72*, 163–174.
38. Jiang, H.; Chen, F.; Lagally, M. G.; Denes, F. S. New Strategy for Synthesis and Functionalization of Carbon Nanoparticles. *Langmuir* **2010**, *26*, 1991–1995.
39. Figueiredo, J. L.; Pereira, M. F. R.; Freitas, M. M. A.; Órfão, J. J. M. Modification of the Surface Chemistry of Activated Carbons. *Carbon* **1999**, *37*, 1379–1389.
40. Ros, T. G.; van Dillen, A. J.; Geus, J. W.; Koningsberger, D. C. Surface Oxidation of Carbon Nanofibres. *Chem.—Eur. J.* **2002**, *8*, 1151–1162.
41. Boehm, H. P. Surface Oxides on Carbon and Their Analysis: A Critical Assessment. *Carbon* **2002**, *40*, 145–149.
42. Kundu, S.; Xia, W.; Busser, W.; Becker, M.; Schmidt, D. A.; Havenith, M.; Muhler, M. The Formation of Nitrogen-Containing Functional Groups on Carbon Nanotube Surfaces: A Quantitative XPS and TPD Study. *Phys. Chem. Chem. Phys.* **2010**, *12*, 4351–4359.
43. Zielke, U.; Hüttinger, K. J.; Hoffman, W. P. Surface-Oxidized Carbon Fibers: I. Surface Structure and Chemistry. *Carbon* **1996**, *34*, 983–998.
44. Palmese, G. R.; McCullough, R. L. Kinetic and Thermodynamic Considerations Regarding Interphase Formation in Thermosetting Composite Systems. *J. Adhes.* **1994**, *44*, 29–49.
45. Hens, S. C.; Cunningham, G.; Tyler, T.; Moseenkov, S.; Kuznetsov, V.; Shenderova, O. Nanodiamond Bioconjugate Probes and Their Collection by Electrophoresis. *Diamond Relat. Mater.* **2008**, *17*, 1858–1866.
46. Krueger, A.; Stegk, J.; Liang, Y.; Lu, L.; Jarre, G. Biotinylated Nanodiamond: Simple and Efficient Functionalization of Detonation Diamond. *Langmuir* **2008**, *24*, 4200–4204.
47. Forns, P.; Fields, G. B. The Solid Support. In *Solid-Phase Synthesis: A Practical Guide*; Kates, S. A.; Albericio, F., Eds.; Marcel Dekker, Inc.: New York, 2000; pp 1−78.
48. Nesterenko, P. N.; Fedyanina, O. N. Properties of Microdispersed Sintered Nanodiamonds as a Stationary Phase for Normal-Phase High Performance Liquid Chromatography. *J. Chromatogr. A* **2010**, *1217*, 498–505.
49. Puzyr, A.; Burov, A.; Bondar, V.; Trusov, Y. Neutralization of Aflatoxin B1 by Ozone Treatment and Adsorption by Nanodiamonds. *Nanotechnologies in Russia* **2010**, *5*, 137–141.